JETIR.ORG ISSN: 2349-5162 | ESTD Year : 2014 | Monthly Issue
JOURNAL OF EMERGING TECHNOLOGIES AND INNOVATIVE RESEARCH (JETIR)
An International Scholarly Open Access, Peer-reviewed, Refereed Journal

EXCITATION STRUCTURES TO MICROSTRIP ANTENNA ARRAY FOR REDUCED ISOLATION AND BACK LOBE RADIATION

[1]G. M. Pushpanjali, [2]K. Prahlada Rao, [3]Vani R. M.

[1]Asstistant Professor, [2]Associate Professor, [3]Professor
[1]Department of Physics,
[1]Sangameshwar College (Autonomous), Solapur, India

Abstract : Present work demonstrates the study of microstrip antenna array with electromagnetic band gap structure and defective ground structure. Obtained results shows the reduction of isolation between the radiating elements of microstrip antenna array with said designing structures. Proposed four element microstrip antenna array exhibits improved bandwidth and gain of 64.62 % and 14.9 dB respectively as against the bandwidth and gain of 4.89 % and 6.81 dB of conventional microstrip antenna array. Further, the proposed antenna array is producing good reduction in mutual coupling equal to -31.51, -31.95 and -33.38 dB respectively. Proposed antenna also produces virtual size reduction of 43.39 % and enhanced radiation characteristics. The antenna arrays are designed at 6 GHz which is at super high frequency band. The dielectric substrate FR-4 glass epoxy with the height of 0.16 cm is used to fabricate the presented antennas. Radiating patches of antenna arrays are designed using Mentor Graphics IE3D software and excited by corporate feeding technique. The experimental results of designed antenna are obtained using vector network analyzer.

IndexTerms **- defective ground structure, electromagnetic band gap structure, corporate feeding technique, gain, mutual coupling, radiation pattern, return loss**

I. INTRODUCTION

Nowadays more emphasis is being laid on developing latest and advanced antenna configurations for improved communication and electrical performance. One of the most popular antennas which has gained widespread usage in various applications and fields of research are microstrip antennas. (Constantine A. Balanis, 1997). One of the most appreciable characteristics of these antennas is that impedance matching is very simple. Added to this, they can be easily mounted, possess planar configuration and ease of fabrication. However, these antennas possess narrow bandwidth and high levels of mutual coupling. These antennas consist of a radiating element sitting on top of the dielectric substrate and the lower end is a ground plane. (I. J. Bahl and P. Bhatia, 1980).

Defective ground structure (DGS) is a structure which is placed in the finite ground plane of the microstrip antenna or array. In its simplest terms, DGS represents the removed copper part in the ground plane. These structures are being employed on a large scale citing their usability and prominence in various domains of research, particularly in microstrip antennas and arrays. (Reinhold Ludwig and Pavel Bretchko, 2009). Electromagnetic band gap (EBG) structures are made up of unit cells which are arranged in a desired fashion so that the cells are periodically spaced. The historical background of EBG structures reveals that these structures play a positive role in the enhancement of performance of microstrip antennas and arrays. (FanYang and Yahya Rahmat-Samii, 2009).

In the year 2010, authors have discussed the study of EBG structures loaded in the ground plane, their types, and their behaviour in enhancing the performance of two element microstrip patch antenna arrays. The EBG structures employed are of two dimensional in nature and corporate feeding technique is used to feed the antenna array. The performances of square, circular, star, H and I shape EBG structures are compared. Highest bandwidth of 5.1 % has been achieved using H shape EBG structure. Least amount of mutual coupling (S_{21}) of -30 dB and highest gain of 13.75 dB have been obtained in the case of star EBG structure. (D. N. Elsheak *et al.*, 2010). In the year 2016, authors have discussed the different techniques employed for mutual coupling reduction in microstrip antenna arrays. These are using EBG structures, split ring resonators, EBG – split ring resonators and DGS. Using EBG and split ring resonator between two radiating elements, reduces the mutual coupling more compared to other techniques. The mutual coupling is reduced to more than 42 dB and side lobes by 6 dB. The proposed

antenna with spiral resonator has 5.5 dB reduction in mutual coupling. A 36-dB reduction in mutual coupling is achieved using DGS. (Shruti Dhamankar and Sneha Lopes, 2016).

In the year 2016, authors have proposed and designed a decoupling module which is composed of coupled metamaterial slabs. Bandwidth of 20 MHz and an isolation improvement of 7 dB are produced by loading the decoupling module between the patches. Gains of the antenna without and with decoupling module are 8.8 and 8.6 dB respectively. Half power beam widths in the absence and presence of decoupling module are 73.3 and 71.4 degrees. (Bai Cao Pan *et al*., 2010). In the year 2018, authors have demonstrated the filtering characteristics of a compact triple band stop filter based on complementary split ring resonator. The complementary split ring resonator is implemented on the extended microstrip line and in the ground plane. It is characterized by dual and single bands. The dual band bandstop filter is suppressing bands corresponding to 2.4 and 3.5 GHz (WLAN/WiMax applications) respectively. The single band bandstop filter is suppressing 5.2 GHz band (WLAN application). (Mohssine El Ouahabi *et al*., 2018).

In the year 1987, author has exhibited that if a three-dimensional periodic dielectric structure has an electromagnetic band gap which overlaps the electronic band edge, then spontaneous emission can be rigorously suppressed and also stimulated emission would be absent. There is periodic modulation along the laser axis and therefore a forbidden gap in the electromagnetic dispersion relation. (Eli Yablonovitch, 1987). In the year 2014, authors have designed 2 × 5 EBG structure to reduce mutual coupling between patch antennas of MIMO array. Two microstrip patch antennas are designed for resonance at 5.28 GHz. The conventional MIMO array is fed by coaxial feed and bandwidth is equal to 3 %. The EBG structure is inserted between the two patch antennas and on the surface. Mutual coupling values without and with EBG structure are -22 and -43 dB respectively. By increasing the gap between the unit cells of EBG structure, the resonant frequency of proposed MIMO array is reduced. A gain value of 6.86 dBi is also produced. Moreover, the EBG structure has reduced antenna current from 8.5 A/m to 3.9 A/m, so the coupling is reduced by 50 %. However, the antenna efficiency is reduced from 65 to 53 %. (Mohammad Naser - Moghadasi *et al*., 2014). In the year 2015, authors have designed novel eagle shaped microstrip antenna array with eagle shaped EBG structure placed on the surface and in between the radiating patches.

The measured results depict that a reduction in mutual coupling of 36 dB is achieved in the first band (1.68 – 2.65 GHz) and 22.1 dB in the second band (6.5 – 8.86 GHz) due to the introduction of EBG structure. Moreover, a size reduction of 80 % is achieved. The bandwidths produced are equal to 31.5 and 30.4 % respectively. Appreciable gains of 4 and 6.2 dB are also obtained. The better performance of proposed antenna arrays is further supported by high values of radiation and antenna efficiencies of 96 and 95 % respectively. (Mohamed I. Ahmed *et al*., 2015). In the year 2016, authors have investigated the effects of two dimensional EBG structure (operating at 2.4 GHz) on the performance of microstrip antenna arrays. Taconic (tm) dielectric material is employed as patch substrate. The mutual couplings of the antennas without and with EBG structure are -38.4 and -40.2 dB respectively. The gain of the proposed antenna is 8 % more than the conventional antenna. (F. Benikhlef and N. Boukli-Hacen, 2016). In the year 2016, authors have analyzed the performance of two element microstrip antenna array using periodic L-loading E-shaped EBG structure between the array elements. A mutual coupling reduction of 26 dB is obtained at 2.55 GHz in the presence of EBG structure. The L loading EBG structure has little effect on radiation pattern. The proposed structure also reduces the current effect on the adjacent antenna elements and hence can improve the decoupling between the adjacent antenna elements. (Tao Jiang *et al*., 2016). In the year 2017, authors have analyzed the isolation properties of different EBG structures and compared them in antenna arrays. Mushroom like EBG, fork shaped EBG and proposed structure with vias are designed and fabricated. With one row of mushroom like EBG structure, the mutual coupling is -22.5 dB. An approximately 4 dB reduction in mutual coupling is observed with fork shaped EBG structure. The EBG structure with vias is producing the best isolation of 6 dB. Hence surface waves are best suppressed using proposed structure using vias. (F. Benikhlef and N. Boukli-Hacen, 2017). In the year 2017, authors have designed dual band MIMO antenna system with enhanced isolation. Using a double rectangular DGS, the antenna is resonating at 2.6 and 5.7 GHz with bandwidths of 5.7 and 4.3 % respectively.

The proposed antenna is having high isolation which is stable and around -20 dB over all frequencies. At 2.6 GHz, gain and radiation efficiency are 2.63 dB and 59 %. The corresponding values at 5.7 GHz are 1.6 dB and 39.8 %. MIMO antenna with double side EBG structure is reducing mutual coupling from -20 to -40 dB. At 2.6 GHz the antenna gain and radiation efficiency are improved to 4.25 dB and 68.7 %. At 5.7 GHz, the antenna gain is increased to 1.76 dB and radiation efficiency to 39.8 %. (Duong Thi Thanh Tu *et al*., 2017). In the year 2018, authors have proposed rectangular and circular EBG structures to investigate the antenna performance used in microwave brain imaging system. The return losses produced due to rectangular and circular EBG structures are -40.15 and -49.29 dB respectively. Using circular EBG is producing better bandwidth of 291.6 MHz compared to 275.5 MHz that due to rectangular EBG. Moreover, gains of 6.7 and 6.06 dBi are obtained using circular and rectangular EBG. The specific absorption rates are equal to 0.922 and 0.695 W/Kg, which are lesser than maximum standard surface absorption rate limit of 1.6 and 2 W/kg, which ensures the safety of the considered microwave brain imaging system. (Reefat Inum *et al*., 2018). In the year 2019, authors have designed dual band circular patch MIMO antenna on an EBG surface. Defects are introduced in the rows and columns of the EBG cells. A healthy reduction in mutual coupling equal to 25 dB is generated between the antenna elements. The proposed antenna is operating in 5.71 – 5.97 GHz and 6.31 – 6.54 GHz respectively. The -10 dB impedance bandwidth is extended by 28.9 and 27.8 % at the low and high frequency band. Moreover, the gains are enhanced by 5 and 6.9 dB and the back-lobe radiations are decreased by 15 and 10.3 dB at the resonant frequencies of 5.75 and 6.44 GHz respectively. (Xiaoyan Zhang *et al*., 2019).

In the year 2015, authors have employed swastika slot DGS for controlling higher order harmonics of resonant frequency 5.2 GHz of microstrip antenna array. Two dumb bell shaped DGS are placed below the feed line of microstrip antenna array. In the presence of DGS, the first harmonic frequency at 9.7 GHz is controlled. The DGS is exhibiting band stop characteristic at certain band of frequencies. The proposed antenna array is used for S band applications. (R. A. Pandhare *et al*, 2015). In the year 2016, authors have introduced a simple coplanar waveguide structure in the ground to get efficient mutual coupling reduction. The dielectric substrate used is F_4Mb-2 with dielectric constant of 2.2 and loss tangent of 0.001. Significant improvement of more than 36 dB isolation is produced compared to the conventional microstrip antennas with inter element spacing of less than 0.024λ. The proposed structure also depicts appreciable improvement in side lobe level and main lobe direction. (Xiao-zun Ma *et al*., 2016). In the year 2016, authors have investigated the performances of single and two element

E-plane coupled microstrip antenna array using a DGS. In the absence of DGS, the microstrip antenna is producing bandwidth and gain of 675 MHz and 4.38 dB at the resonant frequency of 9.95 GHz. With DGS, the bandwidth and gain are enhanced to 1.652 GHz and 8.96 dB. When DGS is integrated with antenna array, a miniaturization of 78.97 % is produced. Mutual coupling reduction of 23.71 dB is also produced. (Munish Kumar and Vandana Nath, 2016). In the year 2016, authors have presented an improved method of size reduction with circular polarization using dumbbell shaped DGS. The DGS is etched in the ground plane below the microstrip line. When the DGS is introduced, the resonant frequency of the antenna array is shifted from 10 to 7.5 GHz, thus producing a miniaturization of 43.75 %. At 7.5 GHz the gain is equal to 8.99 dB. In the proposed antenna array, the current density is more concentrated along the DGS in the ground plane and structure array elements on the top face. (Otman Oulhaj *et al*., 2016). In the year 2016, authors have enhanced the performance of 1:2

microstrip array antenna with DGS on its feed line. The centre frequency is considered as 5 GHz. With the introduction of DGS, although the antenna efficiency and radiation efficiency are remaining same, return loss is improved from -47 to -56 dB. The antenna array with DGS has enhanced directivity with very small cost of antenna gain. The proposed antenna also has stable radiation pattern. The antenna can be useful for C band applications. (Swati Gupta and Dhirendra Kumar, 2016). In the year 2017, author has proposed the design of microstrip patch antenna array using T-power divider circuit. Dumbbell shaped DGS is employed between the two antenna elements. The modified antenna array is producing return loss of -21.99 dB at the resonant frequency of 7.64 GHz. The values of gain and directivity at 7.64 GHz are 6.77 and 6.82 dB respectively. (Roopali Bharadwaj, 2017). In the year 2018, authors have demonstrated the improvement in the performance of microstrip patch antenna array using double I shaped slot DGS. The single element antenna with DGS is resonating at 2.4, 3.58 and 5.5 GHz respectively. The bandwidths produced at the three resonant frequencies are 60, 130 and 70 MHz respectively with a gain of 3.3 dB. By incorporating DGS in the two element microstrip antenna array, four resonant frequencies i.e. 2.48, 3.29, 3.57 and 5.51 GHz respectively are yielded. Improved bandwidths of 80, 90, 110 and 180 MHz are produced. The proposed antenna array is useful for wireless applications. (Nilima A. Bodhaye and P. L. Zade, 2018). In the year 2019, authors have proposed a highly miniaturized microstrip antenna array for small wireless device. Miniaturization of 78.63 % is achieved at 2.45 GHz using a new type of DGS. The resonant frequency of the antenna array is shifted from 5.8 to 2.45 GHz. However, the bandwidth of the proposed array is decreased to 157.5 MHz which covers the operating frequency of Industrial Scientific Medical (ISM) band. It is also clearly observed that a maximum current is shown around the feed network and the extremities of the radiating patch at 5.8 GHz. In the presence of DGS, the density of current is concentrating around DGS slots. (Ahmed Ghaloua *et al*., 2019).

The purpose of the present research is to demonstrate the effect of EBG and DGS structures on the performance of microstrip antenna arrays. The objectives of the present research include enhancement of performance of four element microstrip antenna array in terms of bandwidth, mutual coupling, gain and other radiation characteristics. The novelty in this research work is employing both EBG and DGS structures in the microstrip antenna array. In addition, highest bandwidth and gain of 64.62 % and 14.9 dB are produced compared to the previous literature review.

II. DESIGNING, MATERIALS AND METHODS

The four elements conventional microstrip antenna array (FCMAA) consists of four identical radiating patches designed at 6 GHz. FCMAA is fed by corporate feeding method. The shape of the radiating patches is rectangle. The distance between the adjacent antenna elements of FCMAA is λ/4, where λ is the wavelength calculated at the design frequency of 6 GHz. The dielectric substrate used to design FCMAA is FR-4 glass epoxy with dielectric constant of 4.2 and loss tangent of 0.0245. Figure 1 depicts the schematic of FCMAA and is employed to determine the return loss characteristics of FCMAA. All the dimensions of FCMAA are tabulated in Table 1.

Table 1: Dimensions and values of FCMAA

Parameter	Value (mm)
Length of the patch (Lp)	15.73
Width of the patch (Wp)	11.76
Length of the quarter wave transformer (Lt)	6.47
Width of the quarter wave transformer (Wt)	0.47
Length of the 50Ω line (L1)	6.52
Width of the 50Ω line (W1)	3.05
Length of the coupler (Lc)	3.05
Width of the coupler (Wc)	3.05
Length of the 70Ω line (L2)	6.54
Width of the 70Ω line (W2)	1.62
Length of the 100Ω line (L3)	6.56
Width of the 100Ω line (W3)	0.70
Length of the feed line (Lf)	6.52
Width of the feed line (Wf)	3.05

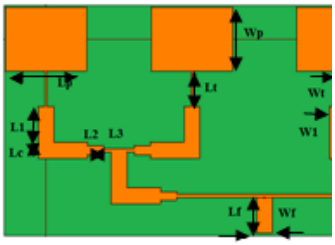

Figure 1: Schematic of FCMAA

To measure the mutual coupling coefficients between the adjacent radiating patches of FCMAA, the four radiating patches are excited separately. The distance between the adjacent elements is same as that maintained in FCMAA. The schematic of the four radiating elements fed independently is shown in Figure 2.

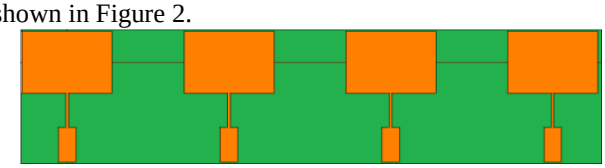

Figure 2: Schematic of setup of FCMAA for mutual coupling measurement

The design of four elements proposed microstrip antenna array (FPMAA) is obtained by modifying the ground plane and surface of FCMAA. The surface of FCMAA is replaced with EBG structure. The EBG structure employed to design FPMAA consists of an array of 3 rows and 2 columns of plus shape patch type unit cells. The unit cell of the EBG structure employed is depicted in Figure 3.

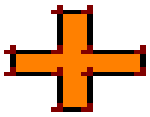

Figure 3: Schematic of plus shape patch type unit cell

The unit cell of the EBG structure depicted in Figure 3 consists of two rectangles intersecting each other at right angles and at their centres. The length and width of each of the rectangles are 5 mm and 1 mm respectively. The EBG structure shown in Figure 4 is placed in between the adjacent radiating patches and on the surface of FCMAA.

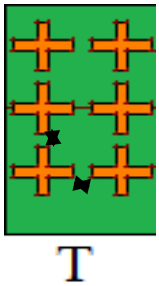

Figure 4: Schematic of plus shape patch type EBG structure

The periodicity of unit cells of plus shape patch type EBG structure is T = 1.5 mm along x-axis and y-axis respectively.

The ground plane of FCMAA is replaced with DGS. The DGS consists of a rotated dumbbell shape structure. The dumbbell structure is rotated by 90^0 from its usual horizontal position. Figure 5 shows the schematic of DGS structure. It consists of two squares which are joined at the centres of one of their sides by a rectangle. The dimensions of each of the squares of the DGS structure are 5 mm × 5 mm respectively. The length and breadth of the rectangle of the DGS structure are 6 mm and 2 mm respectively.

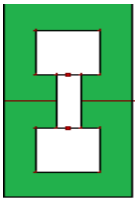

Figure 5: Schematic of rotated dumbbell DGS structure

Figure 6 depicts the schematic of FPMAA. It consists of rotated DGS and plus shape patch type EBG structure in the ground plane and on the surface. The schematic in Figure 6 is used to determine the return loss characteristics of FPMAA.

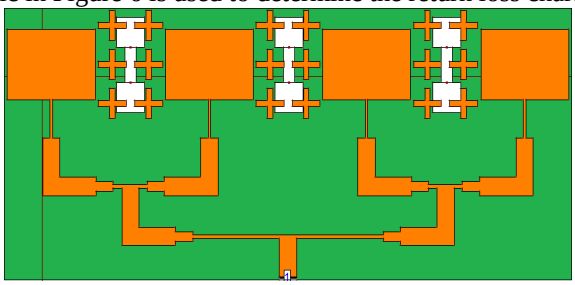

Figure 6: Schematic of FPMMA

To measure the values of mutual coupling of FPMAA, the individual antenna elements of FPMAA are excited separately as shown in Figure 7.

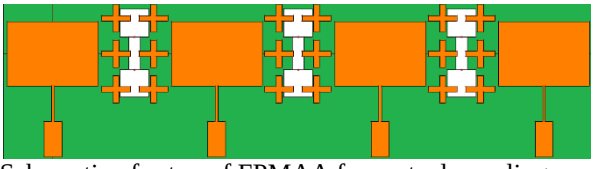

Figure 7: Schematic of setup of FPMAA for mutual coupling measurement

Figures 8, 9, 10 and 11 depict the photographs of the fabricated antennas i.e. FCMAA and FPMAA.

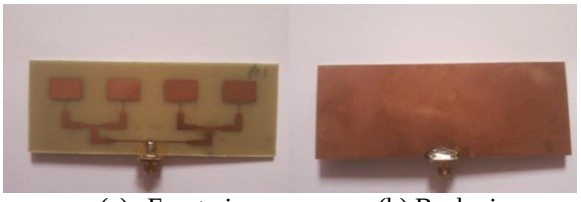

(a) Front view (b) Back view

Figure 8: Photograph of FCMAA

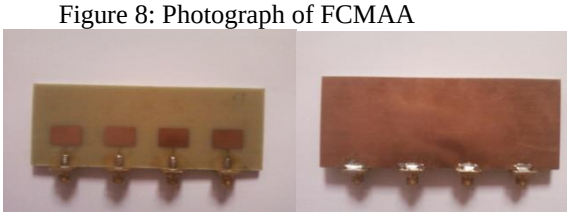

(b) Front view (b) Back view

Figure 9: Photograph of setup of FCMAA for mutual coupling measurement

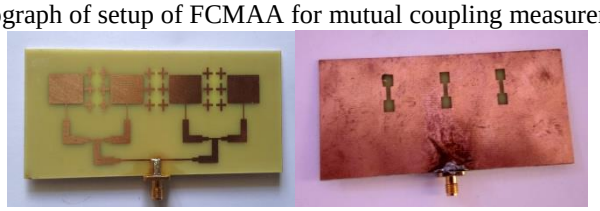

(a) Front view (b) Back view

Figure 10: Photograph of FPMAA

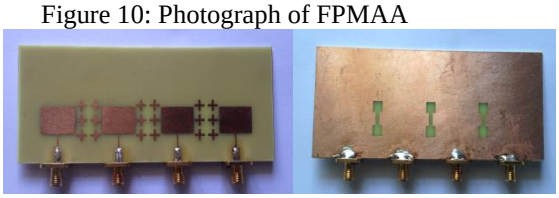

(c) Front view (b) Back view

Figure 11: Photograph of setup of FPMAA for mutual coupling measurement

III. RESULTS AND DISCUSSIONS

The antenna arrays i.e. FCMAA and FPMAA are compared in terms of various parameters. Vector network analyzer is employed to obtain the measured results. Figures 12, 13 and 14 depict the graphs of return loss and mutual coupling versus frequency of FCMAA.

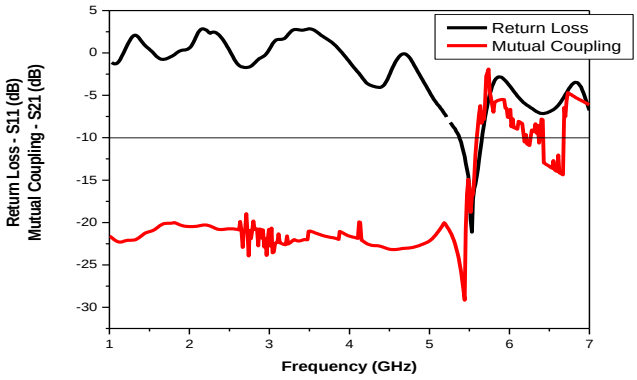

Figure 12: Plot of return loss and mutual coupling – S_{21} versus frequency of FCMAA

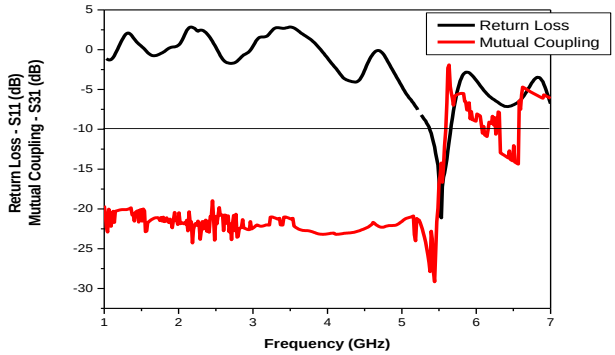

Figure 13: Plot of return loss and mutual coupling – S_{31} versus frequency of FCMAA

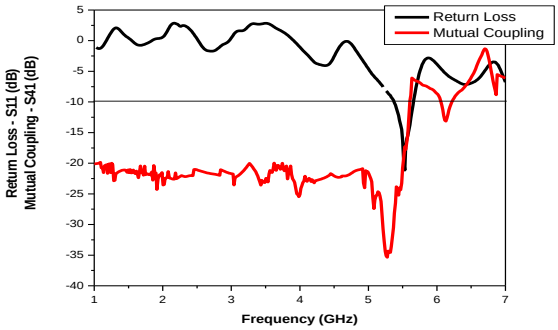

Figure 14: Plot of return loss and mutual coupling – S_{41} versus frequency of FCMAA

Figures 12, 13 and 14 depict that the antenna array FCMAA is resonating at the fundamental frequency of 5.53 GHz with a return loss of -21.06 dB. FCMAA is producing a bandwidth of 273 GHz. The parameter bandwidth (%) is determined by using equation (1).

$$\frac{Bandwidth}{Resonant\ frequency} \times 100\% \quad (1)$$

Thus, the bandwidth (%) of FCMAA is equal to 4.89 %. The mutual coupling parameters measured are S_{21}, S_{31} and S_{41} respectively. At the resonant frequency of 5.53 GHz, the values of these mutual coupling parameters are -16.95, -14.22 and -17.30 dB respectively. These mutual coupling values are high as they are greater than -20 dB. Figures 12, 13 and 14 also show that the plots of return loss and mutual coupling are crossing each other at the resonant frequency of 5.53 GHz. This implies there is huge amount of interference between the transmitting element 1 and the receiving elements 2, 3 and 4 respectively. Hence there is improper transmission and reception of electromagnetic signals between transmitting element 1 and the receiving elements 2, 3 and 4 respectively.

Figures 15, 16 and 17 depict the graphs of return loss and mutual coupling versus frequency of FPMAA.

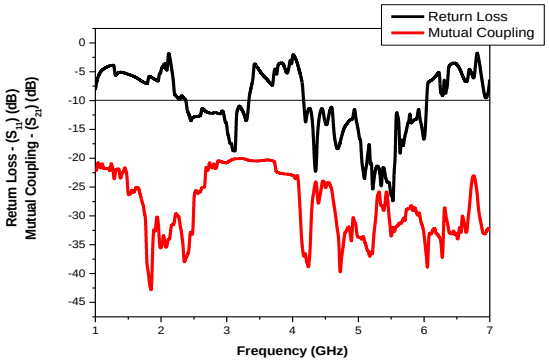

Figure 15: Plot of return loss and mutual coupling – S_{21} versus frequency of FPMAA

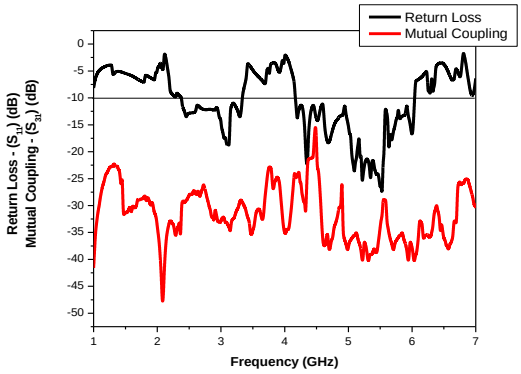

Figure 16: Plot of return loss and mutual coupling – S_{31} versus frequency of FPMAA

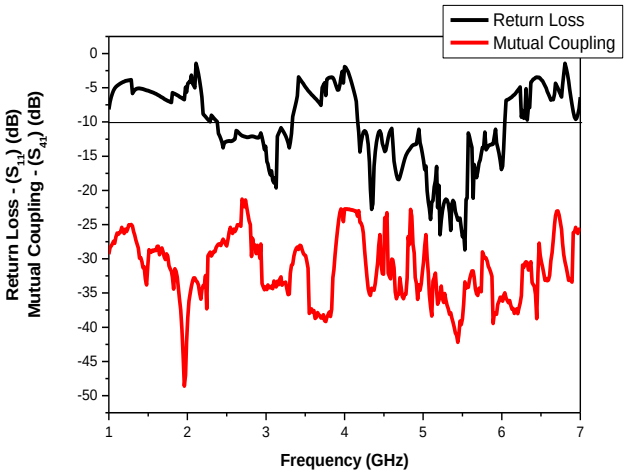

Figure 17: Plot of return loss and mutual coupling – S_{41} versus frequency of FPMAA

From Figures 15, 16 and 17 we see that FPMAA is resonating at dual bands i.e. at 3.13 and 5.53 GHz respectively. FPMAA is producing bandwidths of 970 and 1860 MHz at these two resonant frequencies. Thus, FPMAA is producing an overall bandwidth equal to 64.62 %, which is greater than 4.89 % produced by its counterpart i.e. FCMAA. The measured values of mutual coupling obtained at the resonant frequency of 5.53 GHz are equal to -31.51, -31.95 and -33.38 dB respectively. These values of mutual coupling parameters are reduced compared to that obtained for FCMAA. Also, the graphs of return loss and mutual coupling of FPMAA are not overlapping at the resonant frequency of 5.53 GHz. This confirms the decreased interference level in FPMAA compared to that observed in FCMAA. Hence FPMAA is a better performer than FCMAA in terms of parameters bandwidth and mutual coupling.

The gains of FCMAA and FPMAA are determined by using the equation (2)

$$G = 20\log_{10}\left(\frac{4\pi R}{\lambda}\right) + 10\log_{10}\frac{Pr}{Pt} - Gt \qquad (2)$$

where,

Pt is the transmitted power.

Pr is the received power.

R is the distance between the transmitting and the receiving antennas.

λ is the wavelength at the resonant frequency of 5.53 GHz.

Gt is the gain of the transmitting antenna. Gt is given by the equation (3)

$$Gt = 10\log_{10} Gs \qquad (3)$$

$$Gs = \frac{2\pi ab}{\lambda^2} \qquad (4)$$

where a and b are the length and width of the standard pyramidal horn antenna used as the transmitting antenna. The receiving antenna is the antenna under test i.e. FCMAA and FPMAA respectively. The dimensions a and b are equal to 24 and 14 cm respectively. The distance between the transmitting antenna (standard horn antenna) and the receiving antenna is given by the equation (5)

$$R \geq \frac{2D^2}{\lambda} \qquad (5)$$

where D is the larger dimension of the transmitting antenna. The dimension D is equal to 24cm. The calculated value of R is equal to 71.86m.

Initially considering FCMAA as the receiving antenna, the transmitted and received powers produced are equal to 8.7 µW and 12.414 nW respectively. Hence substituting the corresponding parameter values in equation (2), the value of gain of FCMAA is equal to 6.81 dB. The corresponding values of transmitted and received powers produced by FPMAA are equal to 8.7 µW and 0.079 µW respectively. Substituting the parameter values in equation (2), FPMAA is yielding gain equal to 14.90 dB. Thus, FPMAA is producing increased gain equal to 14.90 dB as compared to 6.81 dB produced by FCMAA. Therefore, FPMAA is a better antenna than FCMAA in terms of gain parameter. The radiation plots of FCMAA and FPMAA are depicted in Figure 18.

The radiation plots in Figure 18 are plotted at the resonant frequency of 5.53 GHz. From Figure 18, we see that without rotated dumbbell shape DGS and plus shape patch type EBG structure, FCMAA is producing forward and backward powers equal to -2 and -4.5 dB respectively. After the introduction of rotated dumbbell shape DGS and plus shape patch type EBG structure, the corresponding powers radiated by FPMAA are 2 and -7 dB respectively. FPMAA is radiating lesser power in the direction of 270^0 and greater power in the direction of 90^0 than FCMAA. That is FPMAA is radiating more power in the desired direction and lesser power in the undesired direction. Hence FPMAA is a better antenna than FCMAA in terms of forward and backward powers. As far as FBR parameter is concerned, the calculated values of FBR of FCMAA and FPMAA are equal to 2.5 and 9 dB respectively. The greater value of FBR of FPMAA than FCMAA implies that FPMAA is radiating in a better way in the forward direction than FCMAA.

Figures 12, 13, 14, 15, 16 and 17 depict that FCMAA and FPMAA are resonating at the fundamental frequencies of 5.53 and 3.13 GHz respectively. The lower fundamental resonant frequency of FPMAA than FCMAA leads to virtual size reduction of FPMAA. To calculate the virtual size reduction (%) produced by FPMAA, equation (6) is employed.

$$\left(\frac{f1-f2}{f1}\right) \times 100 \qquad (6)$$

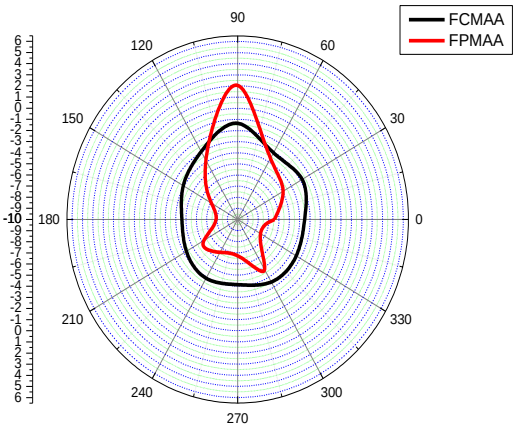

Figure 18: Plots of radiation patterns of FCMAA and FPMAA.

In equation (6), f_1 and f_2 are the fundamental resonant frequencies of FCMAA and FPMAA respectively. Substituting the relevant parameters in equation (6), the virtual size reduction (%) of FPMAA is calculated as equal to 43.39 %.

As FPMAA is performing better than FCMAA in terms of bandwidth, mutual coupling, gain, virtual size reduction, forward power, backward power and FBR, chance FPMAA is a better candidate than FCMAA.

IV. CONCLUSSIONS

The conventional and proposed microstrip antenna arrays have been successfully designed and tested experimentally. The proposed microstrip antenna array is performing better than its counterpart i.e. conventional microstrip antenna array. The plus shape patch type EBG structure and rotated dumb bell DGS structure have successfully played their roles in improving the performance of conventional microstrip antenna array. The proposed microstrip antenna array is useful for applications in C band of the microwave frequency range.

v. ACKNOWLEDGEMENT

The author of the paper would like to acknowledge her gratitude to management of the Shri Sangameshwar Education Societ's, Sangameshwar College, Solapur, The City's first Autonomous College, for granting the "Seed Money for Research" to carry the research work, the obtained results of which is presented in this research paper.

REFERENCES

[1]. Constantine A. Balanis. (1997). Antenna Theory, Analysis and Design, 2nd ed., John Wiley & Sons Inc, New Jersey, 1997.
[2]. Bahl I. J. and Bhartia P. Microstrip Antennas, Artech House, 1980.
[3]. Reinhold Ludwig. and Pavel Bretchko. RF Circuit Design: Theory and Applications, 2nd ed., Pearson, New Jersey, 2009.
[4]. Fan. Yang. and Yahya Rahmat. Samii. Electromagnetic Band Gap Structures in Antenna Engineering, Cambridge University Press, 2009.
[5]. Elsheakh D. N., Iskander M. F., Abdallah E. A. and Elsadek E. A. (2010). Microstrip Array Antenna with New 2D – Electromagnetic Band Gap Structure Shapes to Reduce Harmonics and Mutual Coupling, Progress in Electromagnetic Research C., 12: 13–25.
[6]. Shruti Dhamankar. and Snehal Lopes. (2016). Mutual Coupling Reduction Techniques in Microstrip Patch Antennas: A Survey, International Research Journal of Engineering and Technology., 3 (3): 1064–1069.
[7]. Bai Cao Pan., Wen Xuan Tang., Mei Qing Qi., Hui Feng Ma., Zui Tao. and Tie Jun Cui. (2016). Reduction of the Spatially Mutual Coupling Between Dual – Polarized Patch Antennas Using Coupled Metamaterial Slabs, Scientific Reports, July: 1–8.
[8]. Mohssine El Ouahabi., Alia Zakriti., Mohamed Essaaidi. and Aziz Dkiouak. (2018). A Very Compact of a Triple-Band Bandstop Filter Based on a Complementary Split Ring Resonator, International Journal of Microwave and Optical Technology., 13 (6): 537–543.
[9]. Eli Yablonovitch. (1987). Inhibited Spontaneous Emission in Solid-State Physics and Electronics, Physical Review Letters., 58 (20): 2059–2062.
[10]. Mohammad Naser – Moghadasi., Rahele Ahmadian. Zahra Mansouri., Ferdows B. Zarrabi. and Maryam Rahimi. (2014). Compact EBG Structures for Reduction of Mutual Coupling in Patch Antenna MIMO Arrays, Progress in Electromagnetics Research C., 53: 145–154.
[11]. F. Benikhlef. and N. Boukli-Hacen. (2016). Effects of Two-Dimensional Electromagnetic Bandgap (EBG) Structures on the Performance of Microstrip Patch Antenna Arrays, International Journal of Applied Engineering Research., 11 (11): 7472–7477.
[12]. Tao Jiang., Tianqi Jiao. and Yingsong Li. (2016). Array Mutual Coupling Reduction Using L-Loading E-Shaped Electromagnetic Band Gap Structures, International Journal of Antennas and Propagation., 2016 :1–10.
[13]. F. Benykhlef. and N. Boukli-Hacene. (2017). EBG Structures for Reduction of Mutual Coupling in Patch Antenna Arrays, Journal of Communications Software and Systems., 13 (1): 9–14.
[14]. Duong Thi Thanh Tu., Nguyen Van Hoc., Pham Dinh Son. and Vu Van Yem. (2017). Design and Implementation of Dual-Band MIMO Antenna with Low Mutual Coupling Using Electromagnetic Band Gap Structures for Portable Equipments, International Journal of Engineering and Technology Innovation., 7 (1): 48–60.

[15]. Reefat Inum., Md. Masud Rana., Kamrun Nahar Shushama. and Md. Anwarul Quader. (2018). EBG Based Microstrip Patch Antenna for Brain Tumor Detection Via Scattering Parameters in Microwave Imaging System, International Journal of Biomedical Imaging., 2018: 1–13.

[16]. Xiaoyan Zhang., Yuting Chen., Haitao Ma., Lewei Li. and Huihui Xu. (2019). Design of Defective EBG Structures for Dual-Band Circular Patch MIMO Antenna Applications, AECS Journal., 34 (6): 890–897.

[17]. R. A. Pandhare., P. L. Zade. and M. P. Abegaonkar. (2015). Harmonic Control by Defected Ground Structure on Microstrip Antenna Array, Indian Journal of Science and Technology., 8(35) :1–5.

[18]. Xiao-Zun Ma., Ming-Yang Zhao., De-Feng Zhang. and Peng-Jun Liu. (2016). Mutual Coupling Reduction Between Very Closely Spaced Microstrip Antennas Using CPW Structure, Proc. of MATEC Web of Conferences, ICMIE 2016.

[19]. Munish Kumar. and Vandana Nath. (2016). Analysis of Low Mutual Coupling Compact Multi-Band Microstrip Patch Antenna and its Array Using Defected Ground Structure, Engineering Science and Technology, an International Journal., 19: 866–874.

[20]. Otman Oulhaj., Naima A. Touhami., Mohamed Aghoutane. and Antonio Tazon. (2016). A Miniature Microstrip Patch Antenna Array with Defected Ground Structure, International Journal of Microwave and Optical Technology., 11 (1): 32–39.

[21]. Swati Gupta. and Dhirendra Kumar. (2016). Compact Patch Antenna Array Using Defected Ground Structure on Feedline, International Journal of Computer Applications., 149 (9): 48–51.

[22]. Roopali Bharadwaj. (2017). Design of Micro-Strip Patch Antenna Array Using DGS for ISM Band Applications, Global Journal of Research and Review., 4 (1:7): 1–4. Nilima A. Bodhaye. and P. L. Zade. (2018). Design and Implementation of Multiband Microstrip Patch Array Antenna for Wireless Applications, Journal of Engineering Research and Application., 8(7): 28–32.

[23]. Ahmed Ghaloua., Jamal Zbitou., Larbi El Abdellaoui., Mohamed Latrach., Abdelali Tajmouati. and Ahmed Errkik. (2019). A Novel Configuration of a Miniaturized Printed Antenna Array Based on Defected Ground Structure, International Journal of Intelligent Engineering & Systems., 12(1): 211–220.